Landau Level Spectrum of ABA- and ABC-stacked Trilayer Graphene

Shengjun Yuan[1], Rafael Roldán[1,2], and Mikhail I. Katsnelson[1]
[1] *Institute for Molecules and Materials, Radboud University of Nijmegen, NL-6525AJ Nijmegen, The Netherlands*
[2] *Instituto de Ciencia de Materiales de Madrid, CSIC, Cantoblanco E28049 Madrid, Spain*

(Dated: July 4, 2011)

We study the Landau level spectrum of ABA- and ABC-stacked trilayer graphene. We derive analytic low energy expressions for the spectrum, the validity of which is confirmed by comparison to a π-band tight-binding calculation of the density of states on the honeycomb lattice. We further study the effect of a perpendicular electric field on the spectrum, where a zero-energy plateau appears for ABC stacking order, due to the opening of a gap at the Dirac point, while the ABA-stacked trilayer graphene remains metallic. We discuss our results in the context of recent electronic transport experiments. Furthermore, we argue that the expressions obtained can be useful in the analysis of future measurements of cyclotron resonance of electrons and holes in trilayer graphene.

PACS numbers: 81.05.ue, 71.70.Di, 73.43.Lp, 73.22.Pr

I. INTRODUCTION

Recent experimental realizations of graphene trilayers[1–6] (TLG) have opened the possibility of exploring their intriguing electronic properties, which depend dramatically on the stacking sequence of the graphene layers.[7] The low energy band structure for ABA-stacked TLG consists of one massless and two massive subbands, similar to the spectrum of one single layer (SLG) and one bilayer graphenes (BLG), while ABC trilayer presents approximately cubic bands.[8] Interestingly, when the TLG is subjected to a perpendicular electric field, a gap can be opened for ABC samples,[2,3,9–11] similarly to bilayer graphene,[12] whereas ABA TLG remains metallic with a tunable band overlap.[13]

When a strong magnetic field is applied perpendicular to the TLG planes, the band structure is quantized into Landau levels (LLs). The number of graphene layers as well as their relative orientation (stacking sequence) determine the features of the quantum Hall effect (QHE) in this material, where the Hall conductivity presents plateaus at[14,15]

$$\sigma_{xy} = \pm \frac{ge^2}{h}\left(n + \frac{N}{2}\right), \tag{1}$$

where $N = 3$ is the number of layers, n is the LL index, $g = 4$ is the LL degeneracy due to spin and valley degrees of freedom, $-e$ is the electron charge and h is the Planck's constant. In particular, the plateau structure in σ_{xy} of TLG has been shown to be strongly dependent on the stacking sequence.[2]

In this paper we study the LL quantization of TLG. We obtain analytical expressions for the LL spectrum of TLG with ABA or ABC stacking order. The range of applicability of the analytical results is studied by a comparison to the density of states (DOS) obtained from a numerical solution of the time-dependent Schrödinger equation within the framework of a tight-binding model on the honeycomb lattice.[16–18] We further study the effect of a perpendicular electric field in the LL spectrum, finding that a zero-energy plateau develops in the Hall conductivity only for ABC-stacked graphene, while ABA-stacked graphene remains ungapped.

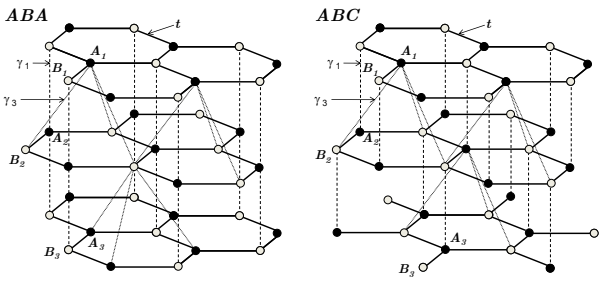

FIG. 1. Atomic structure of ABA- and ABC-stacked trilayer graphene. The intra-layer t and inter-layer γ_1 and γ_3 hopping amplitudes are schematically shown in the figure.

The paper is organized as follows. In Sec. II we obtain analytically the low energy LL spectrum of TLG. The analytic expressions of Sec. II are compared to the DOS numerically obtained from a full tight-binding calculation in the honeycomb lattice in Sec. III. Our main conclusions are summarized in Sec. IV.

II. ANALYTIC DERIVATION OF THE LANDAU LEVEL SPECTRUM

In nature there are two known forms of stable stacking sequence in TLG, namely ABA (Bernal) and ABC (rhombohedral) stacking. The difference between ABA and ABC stacking, schematically shown in Fig. 1, is that the third layer is rotated with respect to the second layer by $-120°$ (so that it will be exactly under the first layer) in ABA stacking, while it is rotated by $+120°$ in ABC stacking.[7,19] In a basis with components of ψ_{A_1}, ψ_{B_1}, ψ_{A_2}, ψ_{B_2}, ψ_{A_3}, ψ_{B_3}, where ψ_{A_i} (ψ_{B_i}) are the envelope functions associated with the probability amplitudes of

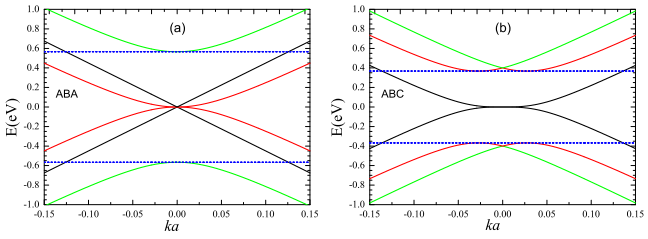

FIG. 2. (Color online) Low energy band structure of ABA- and ABC-stacked trilayer graphene around the K point. We have used the tight-binding parameters $t = 3$ eV and $\gamma_1 = 0.4$ eV. The red dashed lines are a guide to the eye that mark, for the used parameters t and γ_1, the position of the bottom (top) of the upper (lower) bands. The analytic expressions of these bands are given in Appendix A.

the wave functions on the sublattice A (B) of the ith layer ($i = 1, 2, 3$), the effective low energy Hamiltonian of ABA-stacked TLG around the K point is[7]

$$H_{\mathbf{p}} = \begin{pmatrix} 0 & v_{\mathrm{F}}p_- & 0 & 0 & 0 & 0 \\ v_{\mathrm{F}}p_+ & 0 & \gamma_1 & 0 & 0 & 0 \\ 0 & \gamma_1 & 0 & v_{\mathrm{F}}p_- & 0 & \gamma_1 \\ 0 & 0 & v_{\mathrm{F}}p_+ & 0 & 0 & 0 \\ 0 & 0 & 0 & 0 & 0 & v_{\mathrm{F}}p_- \\ 0 & 0 & \gamma_1 & 0 & v_{\mathrm{F}}p_+ & 0 \end{pmatrix}, \quad (2)$$

where $p_\pm = p_x \pm ip_y$, with $\mathbf{p} = (p_x, p_y)$ the two-dimensional momentum operator, and $v_F = 3at/2$ the Fermi velocity of the monolayer graphene, in terms of the in-plane nearest neighbor hopping $t \approx 3$ eV and the carbon-carbon distance $a \approx 1.42$ Å (from now on we use units such that $\hbar \equiv 1 \equiv c$). For the moment, we only include the inter-layer hopping $\gamma_1 \approx 0.4$ eV in Eq. (2). The effective Hamiltonian for K' is obtained by exchanging p_+ and p_-. The effect of far-distant hopping such as γ_3 will be discussed in Appendix C. the Hamiltonian (2) leads to a combination of two linear SLG-like bands [black lines in Fig. 2(a)] and four massive BLG-like bands [red and green lines in Fig. 2(a)].

In the presence of an external perpendicular magnetic field,[20] the canonical momentum $\mathbf{p}$ must be replaced by the gauge-invariant kinetic momentum $\mathbf{p} \to \mathbf{\Pi} = \mathbf{p} + e\mathbf{A}(\mathbf{r})$ where $\mathbf{A}(\mathbf{r})$ is the vector potential, and which obey the commutation relation $[\Pi_x, \Pi_y] = -i/l_B^2$, where $l_B = 1/\sqrt{eB}$ is the magnetic length. Therefore, this allows to introduce the ladder operators $\hat{a} = (l_B/\sqrt{2})\Pi_-$ and $\hat{a}^\dagger = (l_B/\sqrt{2})\Pi_+$, where $\Pi_\pm = \Pi_x \pm i\Pi_y$, and which obey the commutation relation $[\hat{a}, \hat{a}^\dagger] = 1$. As in the usual one-dimensional harmonic oscillator,

$$\hat{a}\,|n\rangle = \sqrt{n}\,|n-1\rangle\,, \hat{a}^\dagger\,|n\rangle = \sqrt{n+1}\,|n+1\rangle\,,$$

where $|n\rangle$ is an eigenstate of the usual number operator $\hat{a}^\dagger\hat{a}|n\rangle = n|n\rangle$, with $n \geq 0$ an integer. Then, the Hamiltonian can be expressed in terms of $\hat{a}$ and $\hat{a}^\dagger$ as

$$\mathcal{H} = \begin{pmatrix} 0 & \Delta_B\hat{a} & 0 & 0 & 0 & 0 \\ \Delta_B\hat{a}^\dagger & 0 & \gamma_1 & 0 & 0 & 0 \\ 0 & \gamma_1 & 0 & \Delta_B\hat{a} & 0 & \gamma_1 \\ 0 & 0 & \Delta_B\hat{a}^\dagger & 0 & 0 & 0 \\ 0 & 0 & 0 & 0 & 0 & \Delta_B\hat{a} \\ 0 & 0 & \gamma_1 & 0 & \Delta_B\hat{a}^\dagger & 0 \end{pmatrix}, \quad (3)$$

where Δ_B is the magnetic energy defined by $\Delta_B = \sqrt{2}v_{\mathrm{F}}/l_B$. Therefore the six-components eigenstates of $\mathcal{H}$ can be reconstructed as $\psi = [c_{A_1}\varphi_{n-1,k}, c_{B_1}\varphi_{n,k}, c_{A_2}\varphi_{n,k}, c_{B_2}\varphi_{n+1,k}, c_{A_3}\varphi_{n-1,k}, c_{B_3}\varphi_{n,k}]^T$, where $c_{A_i}(c_{B_i})$ are amplitudes. If we choose the Landau gauge $\mathbf{A}(\mathbf{r}) = (0, Bx)$, then the wave function of the nth LL $\varphi_{n,k}(x, y)$ is given by[21]

$$\varphi_{n,k}(x,y) = i^n \left(\frac{1}{2^n n!\sqrt{\pi}l_B}\right)^{1/2} e^{iky}e^{-z^2/2}H_n(z)\,, \quad (4)$$

where $z = (x - kl_B^2)/l_B$, $H_n(z)$ is the Hermite polynomial, and $\varphi_{n,k} \equiv 0$ for $n < 0$. Then, the Hamiltonian matrix in the basis of ψ is

$$\begin{pmatrix} 0 & \Delta_B C_1 & 0 & 0 & 0 & 0 \\ \Delta_B C_1 & 0 & \gamma_1 & 0 & 0 & 0 \\ 0 & \gamma_1 & 0 & \Delta_B C_2 & 0 & \gamma_1 \\ 0 & 0 & \Delta_B C_2 & 0 & 0 & 0 \\ 0 & 0 & 0 & 0 & 0 & \Delta_B C_1 \\ 0 & 0 & \gamma_1 & 0 & \Delta_B C_1 & 0 \end{pmatrix}, \quad (5)$$

with $C_1 = \sqrt{n}$ and $C_2 = \sqrt{n+1}$. Eq. (5) has six eigenvalues, which can be easily calculated:

$$E_{n,s} = \pm\frac{1}{\sqrt{2}}[2\gamma_1^2 + (2n+1)\,\Delta_B^2 + s\sqrt{4\gamma_1^4 + 4\,(2n+1)\,\gamma_1^2\Delta_B^2 + \Delta_B^4}]^{1/2}, \quad (6)$$

$$E_{n,0} = \pm\Delta_B\sqrt{n}, \quad (7)$$

with $s = \pm 1$ and $n \geq 0$. The eigenstates corresponding to above LLs are given in Appendix B. Notice that Eq. (6) coincides (apart from a numerical factor $\sqrt{2}$ in front of γ_1) with the LL spectrum of a bilayer graphene,[22] whereas the Eq. (7) corresponds to the LL spectrum of a single layer graphene. This is expected since the low energy band structure of ABA TLG consists of two massless SLG-like bands and four massive BLG-like bands, as it has been discussed above. In Fig. 3(a) we show the LL spectrum Eq. (6)-(7) for ABA TLG obtained for the first 50 LLs of each band (we only show the states with positive energy). As in the zero magnetic field case, there are two sets of BLG-like LLs which disperse roughly linearly with B (the LLs plotted in red and green color), whereas the linearly in $\mathbf{k}$ dispersing SLG-like band leads to a set of $\sqrt{B}$-like LLs (plotted in black) [see Fig. 3(b) for a zoom of the low energy and low magnetic field region of Fig. 3 (a)]. Furthermore, a set of LL crossings occur due to the massless and massive characters of the subbands,

as it has been observed experimentally.[1] Notice that the Landau levels in the low energy part of the spectrum have only $E_{n,-}$ character [see Fig. 3(a) and (b)], unless the magnetic field is very strong. For example, the third low energy Landau level belongs to the set of LLs $E_{n,0}$ when $B \gtrsim 45$ T. On the other hand, the $E_{n,+}$ LLs only appear at an energy $|E| \geq |E_{0,+}| = \sqrt{2\gamma_1^2 + \Delta_B^2}$. In the limit $n\Delta_B^2 \ll \gamma_1^2$, the BLG-like bands Eq. (6) can be simplified to

$$E_{n,-} \approx \pm \frac{v_{\rm F}^2}{l_B^2 \gamma_1} \sqrt{2n\,(n+1)}, \tag{8}$$

which is similar to the commonly used expression for the low energy spectrum of BLG in a weak magnetic field.[14]

Whereas some of the results for the LL spectrum of ABA trilayer graphene has been discussed before,[23] much less effort has been put on understanding the ABC TLG. However, recent experiments have shown the stability of TLG stacked with rhombohedral order, and the possibility of opening a gap by applying a transverse electric field to the sample,[2,3,6] what has activated the interest on TLG with this stacking sequence. The Hamiltonian for ABC-stacked TLG around the K point is

$$H_{\mathbf{p}} = \begin{pmatrix} 0 & v_{\rm F}p_- & 0 & 0 & 0 & 0 \\ v_{\rm F}p_+ & 0 & \gamma_1 & 0 & 0 & 0 \\ 0 & \gamma_1 & 0 & v_{\rm F}p_- & 0 & 0 \\ 0 & 0 & v_{\rm F}p_+ & 0 & \gamma_1 & 0 \\ 0 & 0 & 0 & \gamma_1 & 0 & v_{\rm F}p_- \\ 0 & 0 & 0 & 0 & v_{\rm F}p_+ & 0 \end{pmatrix}. \tag{9}$$

The eigenvalues of Eq. (9) leads, as shown in Fig. 2 (b), to a low energy band structure that consists of a set of six cubic bands, two of them touching each other at the K point, and the other four crossing at an energy $E = \pm\gamma_1$ above (below) the K point. In the following we will obtain the LL spectrum for this case. In a similar manner as for the ABA case, the six-components eigenstates of the Hamiltonian for ABC-stacked TLG can be reconstructed as $\psi = [c_{A_1}\varphi_{n-1,k},\, c_{B_1}\varphi_{n,k},\, c_{A_2}\varphi_{n,k},\, c_{B_2}\varphi_{n+1,k},\, c_{A_3}\varphi_{n+1,k},\, c_{B_3}\varphi_{n+2,k}]^T$, and the Hamiltonian matrix in this case is ($n \geq 0$)

$$\begin{pmatrix} 0 & \Delta_B C_1 & 0 & 0 & 0 & 0 \\ \Delta_B C_1 & 0 & \gamma_1 & 0 & 0 & 0 \\ 0 & \gamma_1 & 0 & \Delta_B C_2 & 0 & 0 \\ 0 & 0 & \Delta_B C_2 & 0 & \gamma_1 & 0 \\ 0 & 0 & 0 & \gamma_1 & 0 & \Delta_B C_3 \\ 0 & 0 & 0 & 0 & \Delta_B C_3 & 0 \end{pmatrix}, \tag{10}$$

with $C_1 = \sqrt{n}$, $C_2 = \sqrt{n+1}$ and $C_3 = \sqrt{n+2}$. The eigenvalues of Eq. (10) are the solutions of the equation

$$E_n^6 + bE_n^4 + cE_n^2 + d = 0, \tag{11}$$

where

$$\begin{aligned} b &= -2\gamma_1^2 - 3\,(1+n)\,\Delta_B^2, \\ c &= \gamma_1^4 + 2\,(1+n)\,\gamma_1^2\Delta_B^2 + \left(2 + 6n + 3n^2\right)\Delta_B^4, \\ d &= -n\,(n+1)\,(n+2)\,\Delta_B^6, \end{aligned} \tag{12}$$

which leads to a LL spectrum for ABC-stacked TLG given by[24]

$$\begin{aligned} E_{n,1} &= \pm\sqrt{2\sqrt{Q}\cos\left(\frac{\theta + 2\pi}{3}\right) - \frac{b}{3}}, \\ E_{n,2} &= \pm\sqrt{2\sqrt{Q}\cos\left(\frac{\theta + 4\pi}{3}\right) - \frac{b}{3}}, \\ E_{n,3} &= \pm\sqrt{2\sqrt{Q}\cos\left(\frac{\theta}{3}\right) - \frac{b}{3}}, \end{aligned} \tag{13}$$

where

$$\theta = \cos^{-1}\left(\frac{R}{\sqrt{Q^3}}\right), \tag{14}$$

$$R = -\frac{b^3}{27} + \frac{bc}{6} - \frac{d}{2}, \tag{15}$$

$$Q = \frac{b^2}{9} - \frac{c}{3}. \tag{16}$$

In Eq. (10), the Landau level index n is required to be nonnegative. However, notice that Eq. (10) admits also eigenstates with real eigenvalues that contain components with $n = -1$. The corresponding eigenenergies can be obtained by setting $C_1 = -1$, $C_2 = 0$ and $C_3 = 1$ in Eq. (10). This leads to three twofold eigenvalues that complement Eq. (13)

$$\begin{aligned} E_{-1,1} &= 0, \\ E_{-1,3} &= \pm\sqrt{\gamma_1^2 + \Delta_B^2}, \end{aligned}$$

where we label the contributions from the last two bands as $E_{-1,3}$, because they have a similar field dependence as the $E_{n,3}$ LLs [see Fig. 3(d)].

In the low magnetic field limit, the Landau level spectrum for ABC-stacked TLG can be approximated by[7,8]

$$E_n \approx \pm\frac{\left(2v_F^2/l_B^2\right)^{3/2}}{\gamma_1^2}\sqrt{n\,(n+1)\,(n+2)}. \tag{17}$$

The positive energy part of the LL spectrum obtained from Eq. (13) is represented in Fig. 3(c). One can distinguish one set of LLs starting from zero energy, which correspond to the low energy band that touches the Dirac point, plus two set of LLs at an energy $\sim \gamma_1$ and which are related to the bands that cross at γ_1 [see Fig. 2(b)]. Whereas the low energy set of LLs can be understood from a standard quantization of a low energy cubic band, the LLs that appears at $E_n \sim \gamma_1$ deserve some discussion [see Fig. 3(d) for a zoom of the low field region of these states]. Most saliently, the hybridization of the upper bands leads to two different sets of LLs. One set of LLs [plotted in green color in Fig. 3(c)-(d)], associated to the inner branches of the hybridized bands [denoted by the green lines in Fig. 2(b)], disperses with an energy $E_n > \gamma_1$ and it is quite similar to that of a SLG. The other set of LLs, associated to the outer branches of the

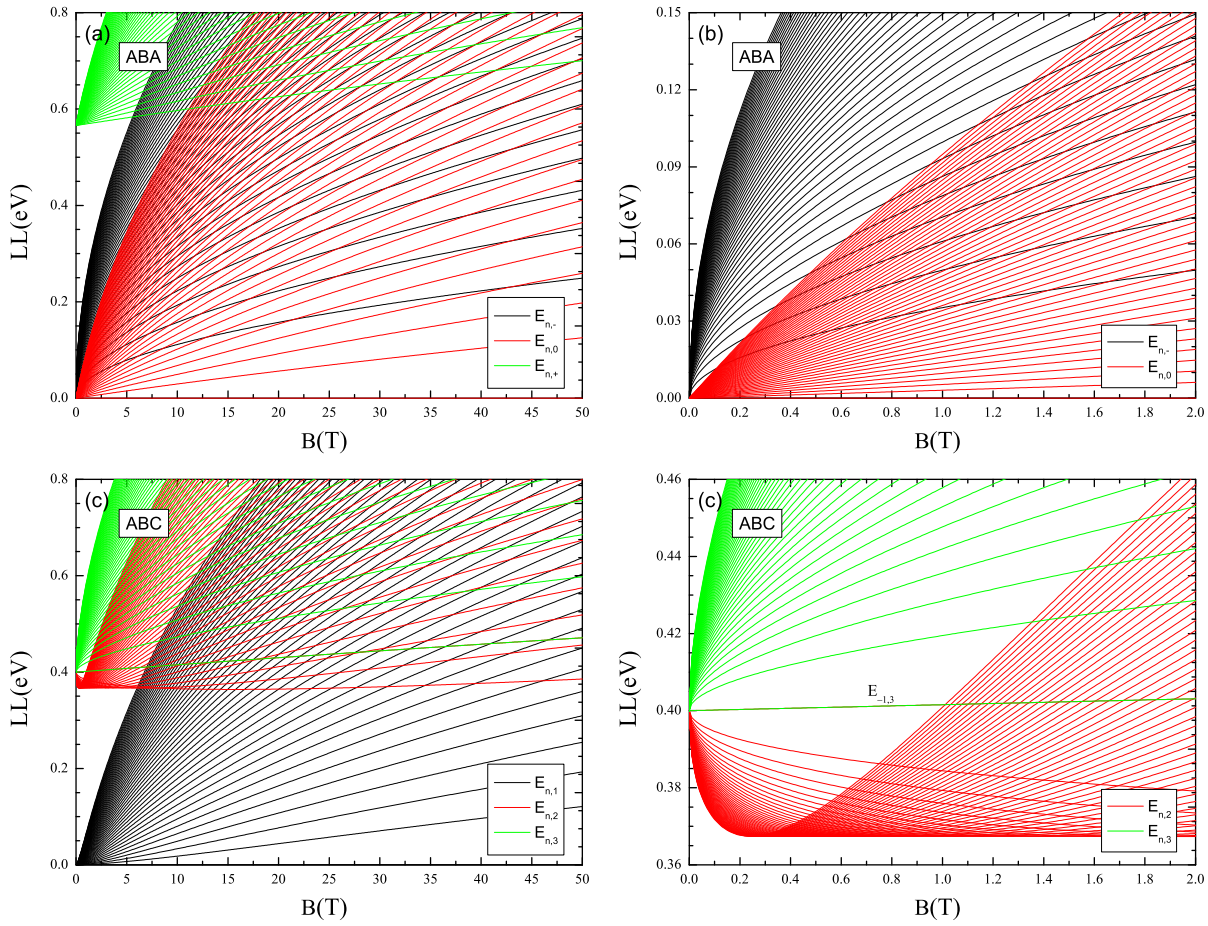

FIG. 3. (Color online) Three band structures in the Landau level spectrum of the ABA- and ABC-stacked trilayer graphene. We have used Eq. (6)-(7) for ABA stacking, and Eq. (13) for ABC stacking. Only the first 50 Landau levels in each band are presented.

hybridized bands [denoted by red lines in Fig. 2(b)], has an energy that first decrease with B until it reaches a minimum value, and then grows in energy as B increases [see the lower set of LLs of Fig. 3(d), which are colored in red]. This behavior is due to the cusp of this branch at $E = \gamma_1$, and resembles the saddle point of the bilayer graphene bands in the presence of a transverse electric field. The effect of the perpendicular electric field in BLG is to open a gap in the spectrum, leading to Mexican hat like bands,[12,25–30] with the corresponding anomalous LL quantization of the band.[22,31,32] Therefore, the LLs associated to the quantization of the lower branches of the hybridized bands in ABC TLG can be obtained, in a first approximation, by using the semiclassical approximation used in Ref. 31 for a biased bilayer graphene. The degeneracy of zero-order Landau level in ABC TLG is three times larger than SLG. This result remains correct also for the case of inhomogenous magnetic field as follows from the index theorem.[33]

III. DENSITY OF STATES FROM A FULL π-BAND TIGHT-BINDING MODEL

In order to check the range of validity of the analytic expressions obtained in Sec. II, in this section we compare the LLs obtained from the equations (6)-(7) and (13) for the low energy spectrum of ABA- and ABC-stacked TLG, respectively, to the density of states (DOS) obtained numerically by solving the time-dependent Schrödinger equation (TDSE) on a honeycomb lattice in the framework of a π-band tight-binding model.[16–18] The effect of an external magnetic field is considered by means of a Peierls substitution

$$t_{mn} \rightarrow t_{mn} e^{ie \int_m^n \mathbf{A}\cdot d\mathbf{l}}, \qquad (18)$$

where t_{mn} is the hopping amplitude between sites m and n of the honeycomb lattice, and $\int_m^n \mathbf{A}\cdot d\mathbf{l}$ is the line integral of the vector potential. A numerical study of the magneto-electronic properties of ABC TLG has been also reported in Ref. 34. In Fig. 4 we compare our analytic results of Eqs. (6)-(7) and (13) with the numerical TDSE

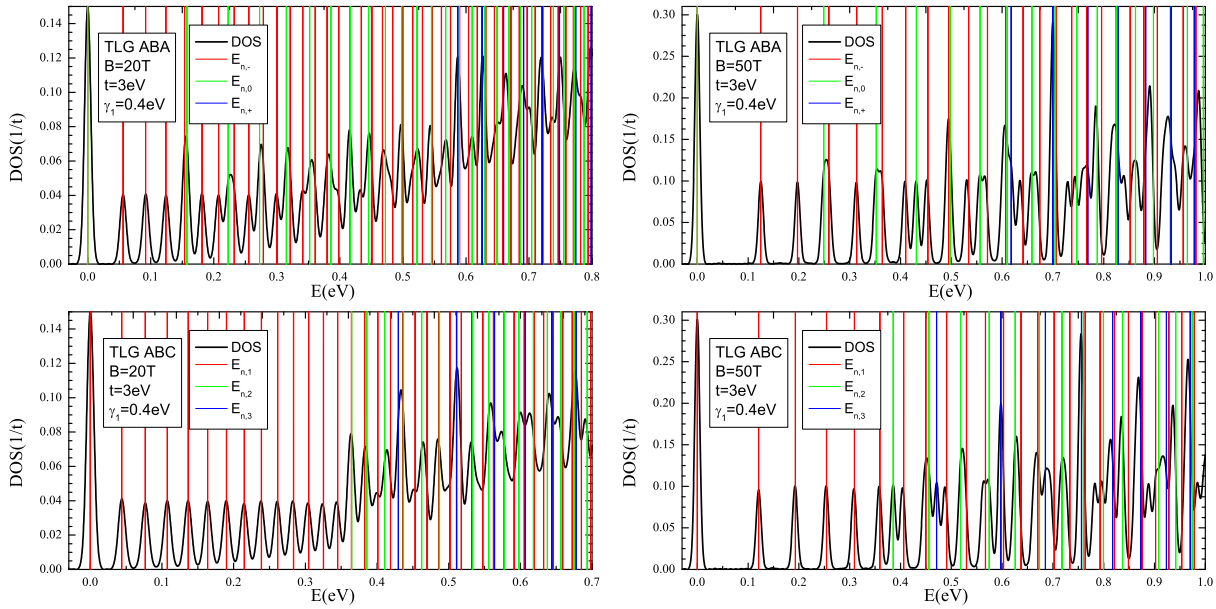

FIG. 4. (Color online) Comparation of the Landau level spectrum obtained from the analytic expressions derived in the text (color lines) and the numerical simulation (black lines) of ABA- and ABC-stacked trilayer graphene. The sample used in the numerical simulations contains 3200×3200 atomic sites in each layer, and we use the periodic boundary conditions in the plane (XY) of graphene layers.

results for the DOS, for two different values of magnetic field. We find a very good agreement between analytic and tight-binding results up to an energy of ~ 0.5 eV. Notice that when a LL crossing occurs, for example of a SLG-like LL crossing with a BLG-like LL in ABA TLG, this leads to an increase of the peak in the DOS. This is, e. g., the reason for the enhanced peaks at $E \approx 0.5$ eV and $E \approx 0.7$ eV in Fig. 4(b), as it can be deduced by following the LL spectrum of Fig. 3(a) at $B = 50$ T. Far from the neutral point, at an energy $E \gtrsim 0.5$ eV the analytic results are shifted to the right of the spectrum, as compared with the numerical TDSE results (see e. g. the peaks corresponding to $E_{n,-}$ for ABA- and $E_{n,1}$ for ABC-stacked TLG, represented by the red vertical lines in Fig. 4). This is due to the fact that the dispersion relation for SLG is not linear anymore, so that higher order terms should be included for a precise reproduction of the position of the LLs.

It is interesting also to check the range of validity of the most commonly used approximated expressions for the LL spectrum of TLG [Eq. (8) for ABA and Eq. (17) for ABC]. Contrary to single layer graphene, for which the LL spectrum behaves as $\sqrt{Bn}$ up to rather high energies (in Ref. 35 it was reported a deviation of only ~ 40 meV at an energy of 1.25 eV), the $B\sqrt{n(n+1)}$ behavior of the BLG-like LLs of ABA TLG as well as the $B^{3/2}\sqrt{n(n+1)(n+2)}$ behavior of ABC TLG are valid only in a rather reduced range of energies in the spectrum. In fact, we see in Fig. 5 that, for the moderate value of magnetic field used for this plot ($B = 20$ T) the approximations Eqs. (8) and (17) fail to capture accurately even the second LL of the spectrum. The deviation is especially important for ABC trilayer graphene, as seen in Fig. 6, where one can see that there are deviations of hundreds of meV between the two results already for low LLs at some intermediate values of magnetic field $\sim 15 - 20$ T. This is somehow expected since recent cyclotron resonance experiments[36,37] on bilayer graphene required the use of the equivalent expression for BLG of Eq. (6), that we have obtained for the BLG-like bands of ABA TLG. Indeed, a good fitting (apart from some possible many-body corrections[38,39]) of the magneto-optical experiments on BLG was achieved by using an expression similar to Eq. (6), with the only tight-binding parameters $\gamma_0 \equiv t$ and γ_1. Therefore, we expect that the analytic expressions Eqs. (6)-(7) and (13) that we have obtained can be useful when analyzing future cyclotron resonance experiments of ABA- and ABC-stacked trilayer graphene.

Furthermore, motivated by recent transport measurements on TLG, which have revealed the strongly stacking dependent quantum Hall effect in this material,[1–6] we have calculated the Hall conductivity for the two stacking sequences of TLG, considering also the effect of a transverse electric field in the spectrum. Here the Hall conductivity σ_{xy} is calculated by using the Kubo formula[40]

$$\sigma_{xy} = -\frac{n_s ec}{B} + \Delta\sigma_{xy}, \tag{19}$$

where the charge density $n_s = \int_0^E \rho(E)\, dE$ is obtained by integration of the DOS $\rho(E)$ calculated from the TDSE

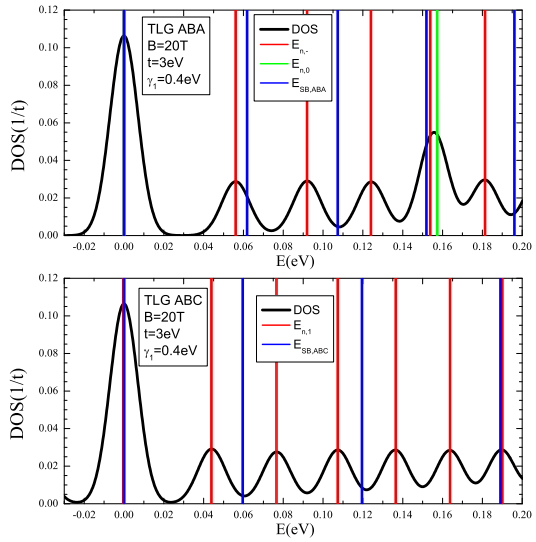

FIG. 5. (Color online) Landau level spectrum of (a) ABA- and (b) ABC-stacked trilayer graphene at $B = 20$ T obtained from the numerical solution of the TDSE using a π-band tight-binding model (black lines). In (a) the TDSE results is compared to the results from the analytic expression $E_{n,-}$ (red vertical lines) and $E_{n,0}$ (green vertical lines) from Eq. (6)-(7), and to the approximation Eq. (8). In (b), the TDSE DOS are compared to the analytic result for $E_{n,1}$ from Eq. (13), and to the approximation Eq. (17) (blue line).

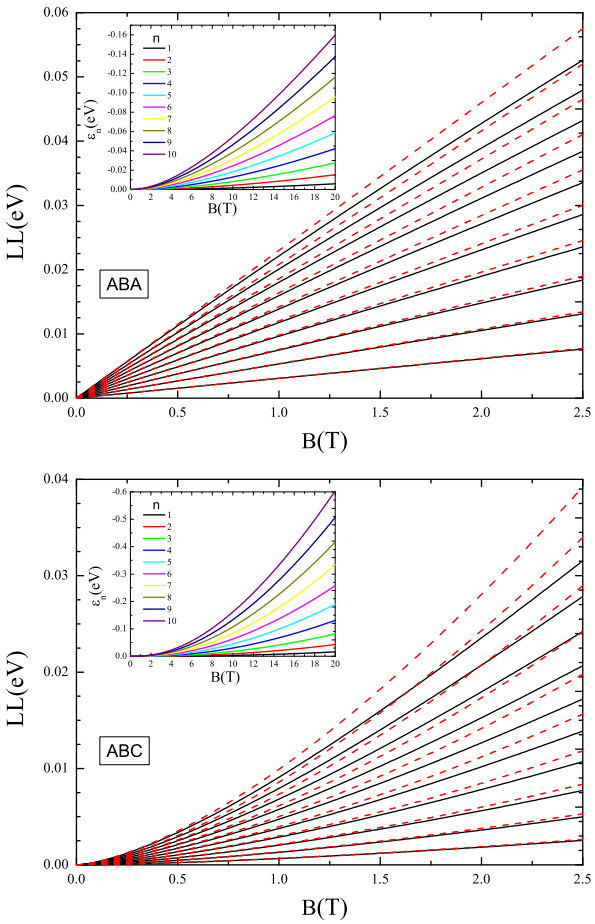

FIG. 6. (Color online) Comparation of the analytic results for the first ten Landau levels obtained from Eqs. (6)-(7) and (13) for ABA- and ABC-stacked graphene, respectively (black solid lines) and the approximations Eqs. (8) and (17) (red dashed lines). The inset panels are the difference between Eq. (6)-(13) and the commonly used approximations Eqs. (8)-(17). Notice the different range of magnetic fields used in the inset with respect to the main figures.

and π-band tight-binding method, and $\Delta\sigma_{xy}$ is a correction due to scattering of electrons with impurities,[17] and which is zero in the clean limit considered here. In Fig. 7, we show the Hall conductivity of ABA- and ABC-stacked TLG with or without an external electric field. In the absence of any bias, the Hall conductivity for the two cases is similar, with plateaus at $\nu = \pm 6, \pm 10, \pm 14, ...$ However, the structure of σ_{xy} is different when we consider the effect of a transverse electric field, which is accounted for here by adding a different (nonzero) on-site potential on the top and the bottom layers, namely, $\Delta_1/2$ on the top layer and $-\Delta_1/2$ on the bottom layer. The main difference between ABA- and ABC-stacked TLG in the presence of a transverse bias is that it leads to a gap opening in the case of ABC-stacking, while the ABA-stacked TLG remains gapless, as it has been observed experimentally.[2] In fact, the opening of the gap and the corresponding insulating state leads to the appearance of a zero energy plateau in the Hall conductivity in ABC TLG, plateau which is absent in ABA TLG, as shown in Fig. 7 for different values of Δ_1. On the other hand, the position of the plateaus depends very much on the value of the induced difference potential Δ_1. For a small bias leading to $\Delta_1 = 0.15$ eV, we find plateaus for ABA TLG at $\nu = \pm 2, \pm 4, \pm 6, \pm 10, \pm 14, ...,$ whereas a higher value, $\Delta_1 = 0.3$ eV leads to plateaus at $\nu = \pm 2, \pm 6, \pm 8, \pm 12, \pm 14, ...$ On the other hand, whereas $\Delta_1 = 0.15$ eV leads to plateaus for ABC at all even values of ν (including $\nu = 0$), some of the plateaus are missing for a higher value of bias, $\Delta_1 = 0.3$ eV, for which we find plateaus at $\nu = 0, \pm 2, \pm 4, \pm 6, \pm 12, \pm 16, ...$ In fact, a more deep understanding of the Hall conductivity of TLG would require further analysis, which is beyond the scope of this work. Furthermore, we emphasize that even experimentally, there is no consensus so far about the structure of the quantum Hall plateaus in trilayer graphene, having been found different structures for almost every transport measurement.[2,4–6]

IV. CONCLUSIONS

In conclusion, we have derived analytic expressions for the Landau level spectrum of trilayer graphene. The two stable stacking sequence, ABA (Bernal) and ABC (rhom-

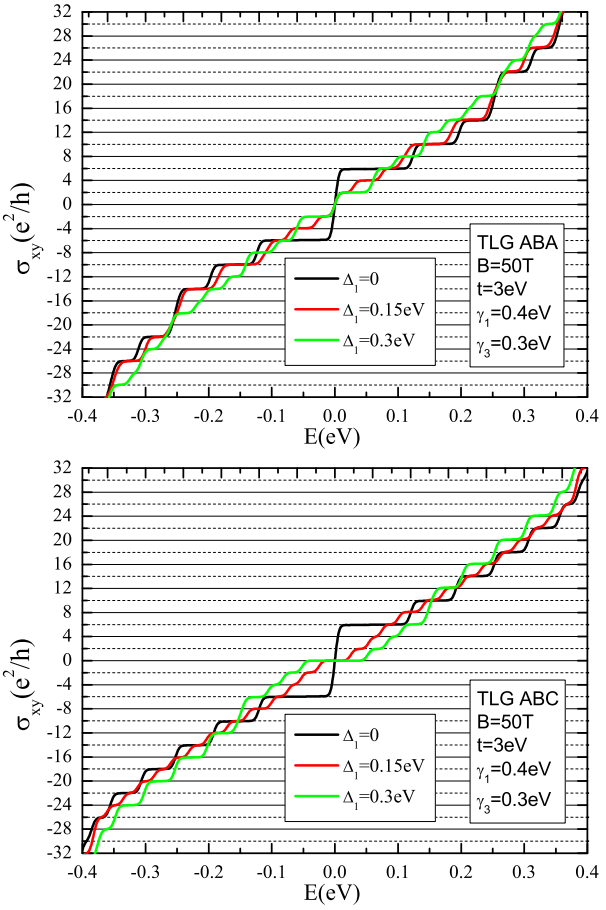

FIG. 7. (Color online) Hall conductivity of ABA- and ABC-stacked trilayer graphene with different values of Δ_1 induced by a transverse electric field.

bohedral) have been considered. The LL spectrum for ABA TLG is composed by a set of bilayer graphene-like LLs, which disperse at low energies as B, and a set of single layer graphene-like LLs, which disperse as $\sqrt{B}$. The different character of the bands lead to a series of LL crossings, which has been observed experimentally.[1] On the other hand, the six cubic bands of ABC TLG leads to a rather peculiar LL quantization of the spectrum. Whereas the bands that touch the Dirac point lead to a set of $B^{3/2}$ LLs, the hybridization between the two bands that cross each other at $E = \gamma_1$ leads to one set of massless like LLs (with energy $E \geq \gamma_1$), and a set of LLs which present a minimum and then grows with B, associated to the lower branch of the hybridized bands. The presence of the minimum on this set of LLs is associated to the presence of a cusp in this branch of the spectrum, in a similar manner as the Mexican hat like dispersion of a biased bilayer graphene.

The range of validity of our analytical results is checked by comparing the LL spectrum obtained in the continuum approximation to the density of states obtained from the numerical solution of the time dependent Schrödinger equation of a π-band tight-binding model on the honeycomb lattice. We find very good agreement between the numerical solution and the analytic approximation for the spectrum up to an energy of ~ 500 meV. However, we show that the most commonly used approximations for the spectrum of TLG, for which the BLG-like LLs of ABA TLG disperse as $B\sqrt{n(n+1)}$ and the LLs for TLG disperse as $B^{3/2}\sqrt{n(n+1)(n+2)}$, fail to capture even the lower LLs already for moderate magnetic fields of ~ 20 T. Therefore, we believe that our results maybe useful for the analysis of future magneto-optical measurements, which has been successfully applied to study the LL spectrum of SLG[41,42] and BLG.[36,37]

Finally, we have calculated the Hall conductivity of TLG by means of the Kubo formula. The inclusion of a transverse electric field leads to a gap opening in ABC TLG, whereas ABA TLG remains metallic. This effect is seen by the appearance of a zero energy plateau only for ABC stacking, in agreement with recent transport experiments.[2,4–6]

V. ACKNOWLEDGEMENT

The authors thank useful conversations with E. V. Castro, E. Cappelluti and F. Guinea. The support by the Stichting Fundamenteel Onderzoek der Materie (FOM) and the Netherlands National Computing Facilities foundation (NCF) are acknowledged. We thank the EU-India FP-7 collaboration under MONAMI and the grant CONSOLIDER CSD2007-00010.

Appendix A: Band structure of ABA and ABC trilayer graphene in the absence of magnetic field

In the absence of a magnetic field, the Hamiltonian of ABA-stacked TLG around the K point is given in Eq. (2), with eigenenergies given by

$$E_s = \pm[\gamma_1^2 + v_F^2k^2 + s\sqrt{\gamma_1^4 + 2\gamma_1^2v_F^2k^2}]^{1/2},\ s = \pm 1$$
$$E_0 = \pm v_F k. \qquad \text{(A1)}$$

Similarly, for ABC-stacked TLG, the Hamiltonian Eq. (9) leads to the eigenvalue problem

$$E^6 - \left(2\gamma_1^2 + 3v_F^2k^2\right)E^4 + \left(\gamma_1^4 + 2\gamma_1^2v_F^2k^2 + 3v_F^4k^4\right)E^2 - v_F^6k^6 = 0, \qquad \text{(A2)}$$

the solutions of which take the form of Eq. (13) with the new quantities $b = -2\gamma_1^2 - 3v_F^2k^2$, $c = \gamma_1^4 + 2\gamma_1^2v_F^2k^2 + 3v_F^4k^4$ and $d = -v_F^6k^6$. In fact, Eq. (A2) can be decomposed into the two equations:

$$E^3 + v_Fk E^2 - \left(\gamma_1^2 + v_F^2k^2\right)E - v_F^3k^3 = 0, \qquad \text{(A3)}$$

$$E^3 - v_Fk E^2 - \left(\gamma_1^2 + v_F^2k^2\right)E + v_F^3k^3 = 0, \qquad \text{(A4)}$$

the solutions of which are

$$
\begin{aligned}
E_{\alpha,s} &= 2\sqrt{Q}\cos\left(\frac{\theta+2\pi}{3}\right) - s\frac{v_F k}{3},\\
E_{\beta,s} &= 2\sqrt{Q}\cos\left(\frac{\theta+4\pi}{3}\right) - s\frac{v_F k}{3},\\
E_{\gamma,s} &= 2\sqrt{Q}\cos\left(\frac{\theta}{3}\right) - s\frac{v_F k}{3},
\end{aligned}
\tag{A5}
$$

where $s = \pm 1$ correspond to the solutions of Eq. (A3) and (A4) respectively, in terms of the new parameters

$$\theta = \cos^{-1}\left(\frac{sR}{\sqrt{Q^3}}\right), \tag{A6}$$

$$R = \frac{8v_F^3k^3}{27} - \frac{v_F k\gamma_1^2}{6}, \tag{A7}$$

$$Q = \frac{3\gamma_1^2 + 4v_F^2k^2}{9}. \tag{A8}$$

Appendix B: Wave functions of ABA trilayer graphene

From the matrix Hamiltonian Eq. (3) one can calculate the eigenstates of the ABA TLG. They are given by

$$
\psi_{n,s}(x,y) = \begin{bmatrix}
\pm\left\{\frac{n{\Delta_B}^2 - E_{n,s}^2}{\sqrt{n}E_{n,s}\Delta_B} - \frac{E_{n,s}}{\sqrt{n}\Delta_B}\left[1 - \frac{(1+n)\Delta_B^2\left(n\,{\Delta_B}^2 - E_{n,s}^2\right)}{{\gamma_1}^2E_{n,s}^2} \pm \frac{E_{n,s}^2 - n{\Delta_B}^2}{{\gamma_1}^2}\right]\right\}\varphi_{n-1,k}(x,y)\\
\left[-1 + \frac{(1+n)\Delta_B^2\left(n\,{\Delta_B}^2 - E_{n,s}^2\right)}{{\gamma_1}^2E_{n,s}^2} \pm \frac{n{\Delta_B}^2 - E_{n,s}^2}{{\gamma_1}^2}\right]\varphi_{n,k}(x,y)\\
\pm\left(\frac{E_{n,s}}{\gamma_1} - \frac{n{\Delta_B}^2}{\gamma_1 E_{n,s}}\right)\varphi_{n,k}(x,y)\\
\left(\frac{\sqrt{1+n}\Delta_B}{\gamma_1} - \frac{n\sqrt{1+n}{\Delta_B}^3}{\gamma_1 E_{n,s}^2}\right)\varphi_{n+1,k}(x,y)\\
\pm\frac{\sqrt{n}\Delta_B}{E_{n,s}}\varphi_{n+1,k}(x,y)\\
\varphi_{n+2,k}(x,y)
\end{bmatrix},
\tag{B1}
$$

and

$$
\psi_{n,0} = \begin{bmatrix}
\mp\varphi_{n-1,k}(x,y)\\
-\varphi_{n,k}(x,y)\\
0\\
0\\
\pm\varphi_{n+1,k}(x,y)\\
\varphi_{n+2,k}(x,y)
\end{bmatrix}.
\tag{B2}
$$

Notice that the states with the eigenvalues $E_{n,0}$ are the surface states which are located only on the top and bottom layers, and these surface states in each layer have the same expressions as the single-layer graphene.

Appendix C: Effect of γ_3 in the DOS

In this appendix we study the effect of considering, besides t and γ_1, the inter-layer hopping amplitude γ_3 in the spectrum (see Fig. 1). In Fig. 8, we compare the Landau level spectrum and Hall conductivity of ABA- and ABC-stacked TLG with and without γ_3. Here we use $\gamma_3 = 0.3$ eV as it is in the nature graphite.[43,44] For the considered magnetic field, the effect of γ_3 in the spectrum is negligible, as seen in Fig. 8. Therefore, trigonal warping has very small effect to the low energy spectrum of the Landau levels in the presence of high magnetic field. In fact, this is also the case in bilayer graphene, where the LL spectrum can be adequately described by neglecting γ_3 over the field range where $l_B^{-1} > \frac{3}{2}a\gamma_3 m$ (where $m \approx 0.054m_e$ is the effective mass in the bulk graphite).[14] In our calculations, the DOS and Hall conductivity are almost the same, as it is shown in Fig. 8.

[1] T. Taychatanapat, K. Watanabe, T. Taniguchi, and P. Jarillo-Herrero, Nature Physics (2011), arXiv:1104.0438.

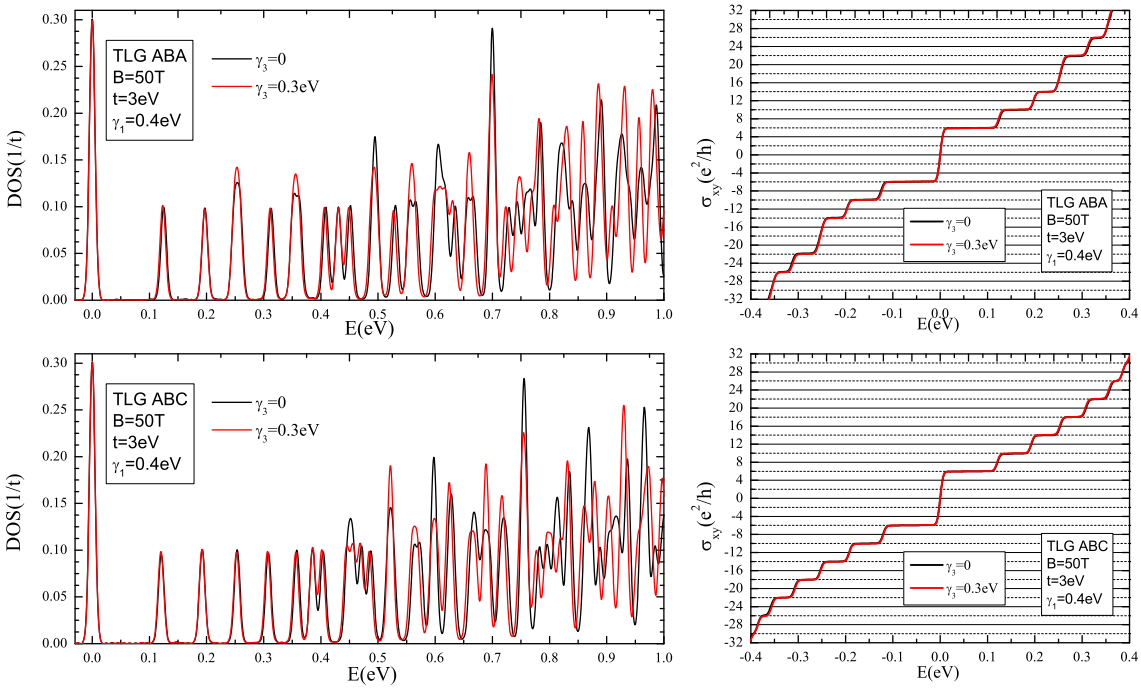

FIG. 8. (Color online) Comparison of the Landau level spectrum and Hall conductivities of ABA- and ABC-stacked trilayer graphene with (red lines) or without (black lines) considering the interlayer hopping parameter γ_3.

[2] W. Bao, L. Jing, Y. Lee, J. V. Jr., P. Kratz, D. Tran, B. Standley, M. Aykol, S. B. Cronin, D. Smirnov, M. Koshino, E. McCann, M. Bockrath, and C. Lau, (2011), arXiv:1103.6088.

[3] C. H. Lui, Z. Li, K. F. Mak, E. Cappelluti, and T. F. Heinz, (2011), arXiv:1105.4658.

[4] A. Kumar, W. Escoffier, J. M. Poumirol, C. Faugeras, D. P. Arovas, M. M. Fogler, F. Guinea, S. Roche, M. Goiran, and B. Raquet, (2011), arXiv:1104.1020.

[5] L. Zhang, Y. Zhang, J. Camacho, M. Khodas, and I. A. Zaliznyak, (2011), arXiv:1103.6023.

[6] S. H. Jhang, M. F. Craciun, S. Schmidmeier, S. Tokumitsu, S. Russo, M. Yamamoto, Y. Skourski, J. Wosnitza, S. Tarucha, J. Eroms, and C. Strunk, (2011), arXiv:1106.4995.

[7] F. Guinea, A. H. Castro Neto, and N. M. R. Peres, Phys. Rev. B **73**, 245426 (2006).

[8] M. Koshino and E. McCann, Phys. Rev. B **80**, 165409 (2009).

[9] A. A. Avetisyan, B. Partoens, and F. M. Peeters, Phys. Rev. B **79**, 035421 (2009).

[10] A. A. Avetisyan, B. Partoens, and F. M. Peeters, Phys. Rev. B **81**, 115432 (2010).

[11] F. Zhang, B. Sahu, H. Min, and A. H. MacDonald, Phys. Rev. B **82**, 035409 (2010).

[12] E. V. Castro, K. S. Novoselov, S. V. Morozov, N. M. R. Peres, J. M. B. L. dos Santos, J. Nilsson, F. Guinea, A. K. Geim, and A. H. C. Neto, Phys. Rev. Lett. **99**, 216802 (2007).

[13] M. F. Craciun, S. Russo, M. Yamamoto, J. B. Oostinga, A. F. Morpurgo, and S. Thrucha, Nat. Nanotechnol. **4**, 383 (2009).

[14] E. McCann and V. I. Fal'ko, Phys. Rev. Lett. **96**, 086805 (2006).

[15] H. Min and A. H. MacDonald, Phys. Rev. B **77**, 155416 (2008).

[16] A. Hams and H. De Raedt, Phys. Rev. E **62**, 4365 (2000).

[17] S. Yuan, H. De Raedt, and M. I. Katsnelson, Phys. Rev. B **82**, 115448 (2010).

[18] S. Yuan, H. De Raedt, and M. I. Katsnelson, Phys. Rev. B **82**, 235409 (2010).

[19] M. Koshino, Phys. Rev. B **81**, 125304 (2010).

[20] For a recent review on the electronic properties of graphene in a magnetic field, see. M. O. Goerbig, (2010), arXiv:1004.3396.

[21] M. Koshino and T. Ando, Phys. Rev. B **77**, 115313 (2008).

[22] J. M. Pereira, F. M. Peeters, and P. Vasilopoulos, Phys. Rev. B **76**, 115419 (2007).

[23] M. Koshino and E. McCann, Phys. Rev. B **83**, 165443 (2011).

[24] See e.g. , G. Birkhoff, and S. M. Lane, *A Survey of Modern Algebra, 5th ed.* (New York: Macmillan, 1996).

[25] E. McCann, Phys. Rev. B **74**, 161403 (2006).

[26] H. Min, B. Sahu, S. K. Banerjee, and A. H. MacDonald, Phys. Rev. B **75**, 155115 (2007).

[27] Y. Zhang, T.-T. Tang, C. Girit, Z. Hao, M. C. Martin, A. Zettl, M. F. Crommie, Y. R. Shen, and F. Wang, Nature **459**, 820 (2009).

[28] K. F. Mak, C. H. Lui, J. Shan, and T. F. Heinz, Phys. Rev. Lett. **102**, 256405 (2009).

[29] A. B. Kuzmenko, E. van Heumen, D. van der Marel, P. Lerch, P. Blake, K. S. Novoselov, and A. K. Geim, Phys. Rev. B **79**, 115441 (2009).

[30] D. Wang and G. Jin, Euro. Phys. Lett. **92**, 57008 (2010).

[31] L. M. Zhang, M. M. Fogler, and D. P. Arovas, (2010), arXiv:1008.1418.
[32] M. Koshino, (2011), arXiv:1105.5919.
[33] M. I. Katsnelson and M. F. Prokhorova, Phys. Rev. B **77**, 205424 (2008).
[34] C. Ho, Y. Ho, Y. Chiu, Y. Chen, and M. Lin, Annals of Physics **326**, 721 (2011).
[35] P. Plochocka, C. Faugeras, M. Orlita, M. L. Sadowski, G. Martinez, M. Potemski, M. O. Goerbig, J.-N. Fuchs, C. Berger, and W. A. de Heer, Phys. Rev. Lett. **100**, 087401 (2008).
[36] E. A. Henriksen, Z. Jiang, L.-C. Tung, M. E. Schwartz, M. Takita, Y.-J. Wang, P. Kim, and H. L. Stormer, Phys. Rev. Lett. **100**, 087403 (2008).
[37] M. Orlita, C. Faugeras, J. Borysiuk, J. M. Baranowski, W. Strupiński, M. Sprinkle, C. Berger, W. A. de Heer, D. M. Basko, G. Martinez, and M. Potemski, Phys. Rev. B **83**, 125302 (2011).
[38] R. Roldán, J.-N. Fuchs, and M. O. Goerbig, Phys. Rev. B **82**, 205418 (2010).
[39] K. Shizuya, (2011), arXiv:1103.5696.
[40] R. Kubo, J. Phys. Soc. Jpn. **12**, 570 (1957).
[41] M. L. Sadowski, G. Martinez, M. Potemski, C. Berger, and W. A. de Heer, Phys. Rev. Lett. **97**, 266405 (2006).
[42] Z. Jiang, E. A. Henriksen, L. C. Tung, Y.-J. Wang, M. E. Schwartz, M. Y. Han, P. Kim, and H. L. Stormer, Phys. Rev. Lett. **98**, 197403 (2007).
[43] B. Partoens and F. M. Peeters, Phys. Rev. B **74**, 075404 (2006).
[44] A. H. Castro-Neto, F. Guinea, N. M. R. Peres, K. Novoselov, and A. K. Geim, Rev. Mod. Phys. **81**, 109 (2009).